Research Square

Preprints are preliminary reports that have not undergone peer review.
They should not be considered conclusive, used to inform clinical practice,
or referenced by the media as validated information.

Erastin and Rapamycin Synergistically Disrupt Redox Homeostasis and Promote Mitophagy-Associated Cell Death in MCF-7 Breast Cancer Cells)

Suhayla Hamad Shareef
Salahaddin University-Erbil
Shang Ziyad Abdulqadir
Salahaddin University-Erbil
Lina Abdulfatah Abdulrazaq
Salahaddin University-Erbil
Kamal A. Khidir
kak29@leicester.ac.uk

University of Leicester
Adam M. Faraj
Tishk International University-Erbil
Ramyar Hassan Mahmud
University of Sulaimani
Hawro Taha Hamza
Nanakali Teaching Hospital, Ministry of Health
Harem Khdir Awla
Salahaddin University-Erbil
Peshraw Salih Hamadamin
Salahaddin University-Erbil
Khder H. Rasul
Salahaddin University-Erbil

Research Article

Keywords: Breast cancer, Erastin, Rapamycin, Redox imbalance, Mitophagy, Autophagy, Mitochondrial ROS

Posted Date: November 24th, 2026

DOI: https://doi.org/10.21203/rs.3.rs-11173644/v1

License: This work is licensed under a Creative Commons Attribution 4.0 International License.
Read Full License

Additional Declarations: No competing interests reported.

Abstract

Background

Breast cancer progression and resistance to therapy are closely tied to metabolic flexibility and redox adaptation.

Aim

Explore the relationship between redox imbalance, mitophagy activation, and autophagy-mediated cell death in MCF-7 breast cancer cells treated with erastin (ERA), rapamycin (RAPA), or their combination.

Method

MCF-7 cells were exposed to ERA (80 μM), RAPA (100 nM), or ERA + RAPA for 24–72 hours. Cell viability was measured using the MTT assay. Redox status was evaluated by measuring TOS, TAC, GSH/GSSG ratio, NADPH/$NADP^+$ ratio, and antioxidant enzyme activities (GPx, GR, SOD, CAT). Mitophagy and autophagy markers (PINK, PARKIN, LC3-I, LC3-II) were analyzed through Western blotting.

Result

ERA and RAPA decreased cell viability over time, with the combination treatment being the most cytotoxic. The treatments led to increased TOS levels, along with decreased TAC, GSH/GSSG, NADPH/$NADP^+$ ratios, and antioxidant enzyme activities, indicating significant redox disruption. Upregulation of PINK1, Parkin, and BNIP3 suggested activation of both ubiquitin-dependent and receptor-mediated mitophagy pathways. The increased LC3-II/LC3-I ratios indicated enhanced autophagic activity, particularly in the combined treatment group.

Conclusion

ERA and RAPA, especially when used together, cause significant oxidative stress and mitochondrial dysfunction in MCF-7 breast cancer cells. This leads to disruption of the glutathione-NADPH antioxidant system, increased mitochondrial ROS levels, reduced antioxidant enzyme activities, and activation of mitophagy and autophagy signaling pathways. These results underscore the importance of targeting redox vulnerability and mitochondrial dysregulation as potential therapeutic strategies in breast cancer.

1. Introduction

Breast cancer is the most commonly diagnosed malignancy in women globally. It remains a significant cause of cancer-related deaths, despite advancements in treatment. Resistance to traditional therapies, tumor diversity, and metabolic adaptability have led researchers to investigate alternative cell death pathways for potential therapeutic interventions. Recently, ferroptosis and autophagy-dependent cell death have gained attention in breast cancer research due to their unique mechanisms compared to apoptosis, as well as their links to cellular redox balance and mitochondrial function (Liu et al., 2023).

In physiological conditions, cellular redox balance is maintained by regulating the balance between reactive oxygen species (ROS) and antioxidant defense systems (Zandi and Schnug, 2022, Mohammed and Shareef, 2026). In line, mitochondria are the main source of ROS, which can damage cells if not controlled. It produces superoxide as a by-product of oxidative phosphorylation (Yang et al., 2023). Therefore, while intact mitochondria produce physiological ROS, an excess superoxide production can negatively affect the oxidant/antioxidant balance. The redox system provided by mitochondria plays a key role in maintaining this balance, which is mainly marked by the reduced glutathione (GSH)/ glutathione disulfide (GSSG) ratio and NADPH/$NADP^+$ levels (Chandel, 2021, Koju et al., 2022, Darweesh and Alnori, 2025). Thus, any disruption in the GSH/GSSG ratio, NADPH/$NADP^+$ levels, or antioxidant enzyme activity significantly impairs cellular redox balance and initiates a cascade that results in oxidative stress and cell death (Koju et al., 2022). To better understand the issue, one should note that GSH is a key intracellular antioxidant that scavenges ROS and supports glutathione peroxidase (GPx) in detoxifying hydrogen peroxide and lipid peroxides. During this process, GSH is oxidized to GSSG (Sarıkaya and Doğan, 2020). The regeneration of GSH from GSSG relies on glutathione reductase (GR) and NADPH as an electron donor (Sreekumar et al., 2021). Thus, the GSH/GSSG ratio indicates the cell's redox state, while the NADPH/$NADP^+$ ratio determines its antioxidant recycling capacity (Xiao and Loscalzo, 2020).

Autophagy is a cellular process that degrades damaged proteins, aggregates, and organelles to maintain cellular health (Alharbi et al., 2021). It is upregulated in response to oxidative stress and nutrient deprivation (Wu et al., 2020). Autophagosomes form by conjugating LC3-I to phosphatidylethanolamine, leading to cargo degradation in lysosomes (Jarocki et al., 2024). Although autophagy can exert protective effects, excessive autophagy can lead to cell death, especially under oxidative stress (Wang et al., 2023). In cancer, autophagy can act as a tumor suppressor by removing damaged components or as a survival mechanism against therapy and metabolic stress (Chavez-Dominguez et al., 2020). A critical mechanistic bridge between oxidative stress and autophagy is mitophagy. Indeed, mitophagy is a selective autophagic removal of damaged mitochondria (Vargas et al., 2023). It is regulated by two pathways, including the PINK1/Parkin ubiquitin-dependent pathway and receptor-mediated mechanisms involving BNIP3 and NIX (Jee and Cheong, 2023). When mitochondria lose their membrane potential or accumulate too many ROS, PINK1 stabilizes on the outer mitochondrial membrane and recruits Parkin (Barazzuol et al., 2020). This leads to the ubiquitination of mitochondrial proteins and their targeting for autophagy (Zhou et al., 2023). Alternatively, BNIP3/NIX facilitates direct mitochondrial recognition by the autophagic machinery (Yamashita et al., 2024). Although mitophagy is initially protective by preventing

propagation of mitochondrial ROS, persistent oxidative stress may shift this response toward autophagy-dependent cell death (Ma et al., 2020).

Erastin (ERA), a known inducer of ferroptosis, inhibits the cystine/glutamate antiporter system Xc^- (Wang et al., 2020). It reduces cystine uptake, impairs GSH synthesis, and makes cells more vulnerable to oxidative stress (Wang et al., 2021, Guo et al., 2023). In breast cancer studies, ERA has been found to raise intracellular iron levels, increase ROS production, and trigger a form of cell death that is not apoptosis (Sun et al., 2020). Rapamycin (RAPA) is a macrolide compound that selectively inhibits mTORC1, a key regulator of cell growth and metabolism (Liu et al., 2025). RAPA, by blocking mTORC1, triggers autophagy by the ULK1 complex, leading to increased autophagic flux (Tao et al., 2025). Additionally, RAPA affects cellular redox balance by influencing mitochondrial metabolism, ROS production, and antioxidant pathways (Chen et al., 2021). In cancer models, including breast cancer, RAPA alters oxidative stress parameters by modulating mitochondrial activity and metabolic fluxes (Semlali et al., 2022). The current study was designed to explore the interplay between redox imbalance, mitophagy activation, and autophagic cell death in MCF-7 breast cancer cells following exposure to ERA and RAPA, individually and in combination.

2. Materials and Methods

2.1. Cell Culture Conditions

MCF-7 cells were cultured in RPMI-1640 medium with 10% fetal bovine serum, 2 mM L-glutamine, and 1% penicillin-streptomycin at 37°C with 5% CO_2. The medium was changed every 2–3 days, and cells were sub cultured at 70–80% confluence using trypsin-EDTA. Cells between passages 3 and 10 were used for experiments.

2.2 Experimental Design and Treatment Protocol

MCF7 Cells (6×10^3 cells/well) were seeded at 96-well plates for MTT assay. After 24 h of attachment, cells in wells grouped into four experimental groups: Control (vehicle-treated), ERA (80 μM), RAPA (100 nM), and ERA (80 μM) + RAPA (100 nM). Treatments were administered for 24 and 48 hours. Control cells received equivalent volumes of DMSO.

2.3 Cell Viability Assay (MTT)

Cell viability was determined by the MTT assay (Shareef et al., 2026). After treatment with ERA and RAPA, the culture medium was exchanged with fresh medium containing MTT (final concentration of 0.5 mg/mL) and incubated for 4 h at 37°C. The formazan crystals were dissolved in DMSO, and the absorbance was read at 570 nm using a microplate reader. Cell viability was calculated as a percentage compared to the control group.

2.4. Preparation of the cell lysate

Cells were detached using trypsin, followed by the addition of a 2 mL culture medium and collected. The mixture was then centrifuged at 1500 × g for 5 min in a cold centrifuge, and washed 3X with PBS (pH 7.4). The pellet was transferred to an extraction solution containing 20 mM PBS (pH 7) and a protease inhibitor cocktail. The cells were sonicated using a Biosonic IV sonicator for 3 min on ice and centrifuged at 12,000 × g for 10 min in a cold centrifuge. The resulting supernatant was used in subsequent tests.

2.5. Determination of Total Oxidant Status (TOS) and Total Antioxidant Capacity (TAC)

From collected supernatant, TOS and TAC were measured using commercial colorimetric assay kits according to the manufacturer's instructions. TOS concentrations were calculated using the equation $y = 0.0263x + 0.2531$ ($R^2 = 0.95$) from the standard curve. The TAC level was calculated using the equation $y= -0.0065x + 0.5603$ ($R^2= 0.97$).

2.6. Determination of GSH/GSSG Ratio

Reduced and oxidized glutathione levels were quantified using an enzymatic recycling method provided in the commercial assay kit. Total glutathione was measured by preparing GSH standards in extraction buffer (0–50 µM) and diluting cell extracts threefold in extraction buffer. Standards and supernatants were added to a 96-well plate with buffer solution, pre-incubated, and then substrate and enzyme/coenzyme working solutions were added. Absorbance at 412 nm was measured kinetically to calculate total glutathione. For GSSG measurement, standards were prepared similarly (0–25 µM) and supplemented with masking solution. Samples were treated with masking solution, then assayed in the presence of quenching solution. GSH was calculated as (GSH + GSSG) − 2 × GSSG, and the GSH/GSSG ratio was determined.

2.7. Determination of NADPH/$NADP^+$ Ratio

Intracellular NADPH and $NADP^+$ levels were measured using a colorimetric assay kit. Cells were lysed, and the supernatant was collected after centrifugation. Total $NADP^+$+NADPH was quantified by incubating the extract with G6PDH and chromogen solution before measuring absorbance at 450 nm. For NADPH-only measurement, $NADP^+$ was decomposed before the reaction steps. The NADPH/$NADP^+$ Ratio was calculated using the equation $y = 4.0425x + 0.2105$ ($R2 = 0.94$).

2.8. Measurement of Antioxidant Enzyme Activities

Enzymatic activities were determined in cell lysates using commercially available assay kits according to the manufacturer's instructions. The glutathione peroxidase (GPx) activity was assessed based on the NADPH oxidation rate. GPx activity was calculated from the standard curve ($y = 0.0061x + 0.04$; $R^2 = 0.97$). Glutathione reductase (GR) activity was determined by monitoring NADPH consumption. GR activity was calculated from the standard curve ($y = 0.1635x + 0.5122$; $R^2 = 0.96$). Superoxide dismutase (SOD) activity was evaluated by inhibition of superoxide-driven reactions. Each plate included a blank (buffer without sample) and a standard curve with known SOD concentrations. SOD activity was calculated using the formula: SOD Activity (U/mg protein) = [(A blank - A sample) / A blank] × 100 ÷ 50.

Where A blank and A sample are the absorbance values of the blank and sample, respectively. One unit of SOD activity is defined as the amount of enzyme needed to inhibit the chromogen reduction rate by 50%. Catalase (CAT) activity was assessed by measuring the decomposition of hydrogen peroxide. CAT activity was calculated from the standard curve ($y = 0.0074x + 0.3213$, $R^2 = 0.97$). All enzyme activities were normalized to total protein concentration (Mohammed and Shareef, 2026).

2.9. Protein Extraction and Western Blot Analysis

Cells were treated, washed with cold PBS, and lysed in RIPA buffer with protease inhibitors. Protein concentration was determined using the Bradford method. Equal amounts of protein (30–50 µg) were separated by SDS-PAGE and transferred to PVDF membranes. Membranes were blocked with 5% non-fat dry milk, then incubated overnight at 4°C with primary antibodies against PINK, PARKIN, LC3-I, LC3-II, and β-Actin. After washing, membranes were incubated with HRP-conjugated secondary antibodies for 1 h at room temperature. Protein bands were visualized using ECL and quantified with ImageJ software.

2.10. Statistical Analysis

Statistical analyses were conducted using GraphPad Prism. One-way ANOVA with Tukey's post hoc test for multiple group comparisons. Experiments were conducted with at least three independent biological replicates. Enzymatic assays were performed in triplicate, and mean values were used for analysis. Data are presented as mean ± SD. A p-value < 0.05 was considered statistically significant.

3. Results

3.1. Effects of ERA and RAPA on MCF-7 Cell Viability

Results of MTT analysis showed that ERA and RAPA treatment reduced MCF-7 cell viability in both time points. In addition, combined ERA + RAPA treatment further decreased cell viability significantly compared to individual treatments and control, especially at 48 h (Fig. 1).

3.2. Effect of ERA and RAPA on Oxidative Stress Status

In current study, both ERA and RAPA significantly increased TOS levels compared to control as used alone. The ERA + RAPA group had the highest TOS levels compared to control group and use them alone. Regarding TAC, the TAC levels were significantly reduced in ERA-treated cells and RAPA-treated cells when used alone. In addition, co-treatment further decreased TAC compared to individual treatments and control group (Fig. 2).

3.3. Effect of ERA and RAPA on Cellular Redox Homeostasis

Intracellular glutathione homeostasis was significantly disrupted by ERA treatment, leading to a decrease in the GSH/GSSG ratio. RAPA also reduced the ratio, with the ERA + RAPA group showing the

lowest ratio. The NADPH/$NADP^+$ ratio was significantly decreased in ERA-treated cells. RAPA and co-treatment further reduced the ratio (Fig. 3).

3.*4. Effect of ERA and RAPA on Antioxidant Enzyme Activities*

The ERA significantly reduced key antioxidant enzyme activities including GPx, GR, SOD, and CAT compared to control cells. Also, RAPA treatment moderately reduced antioxidant enzyme activities. In addition, the combined treatment group showed the most significant decrease in enzymatic activities compared to single treatments (Fig. 4).

3.5. Effect of ERA and RAPA on Mitophagy-Related Protein Expression

Western blot analysis showed a significant increase in PINK1 and Parkin protein expression in cells treated with ERA compared to controls. RAPA also increased PINK1 and Parkin expression, although to a lesser degree. Interestingly, the ERA + RAPA group had the highest levels of both proteins compared to control, suggesting increased recruitment of mitophagic machinery in response to heightened oxidative stress. Additionally, BNIP3 expression was significantly higher after ERA treatment and further elevated in the combination group, indicating activation of receptor-mediated mitophagy pathways (Fig. 5).

3.6. Induction of Autophagic Flux: Increased LC3-II/LC3-I Ratio

Autophagy activation was assessed by analyzing LC3 conversion. ERA and RAPA treatments significantly increased the LC3-II/LC3-I ratio compared to control, indicating enhanced autophagosome formation. The ERA + RAPA group showed the highest LC3-II/LC3-I ratio, suggesting increased autophagic flux with combined treatment (Fig. 6).

5. Discussion

The MTT assay revealed a time-dependent decrease in cell viability with ERA and RAPA treatments, which was further enhanced when the two chemicals were combined. This suggests that ERA induces redox vulnerability over time by limiting cystine levels (Swanda et al., 2023), while RAPA inhibits mTORC1 to change growth and stress responses (Liu et al., 2025). The increased cytotoxicity in the ERA + RAPA group represents that autophagy activation and metabolic changes can exacerbate cellular stress when antioxidant capacity is compromised. In breast cancer cells, this dual-hit model suggests that ferroptotic pressure and autophagy can synergistically lead to cell death by increasing oxidative stress and disrupting cellular functions (Li et al., 2025, Mahemuti et al., 2026).

Regarding oxidative stress, mitochondrial superoxide levels increase with ERA and RAPA treatments, peaking with combined treatment. Mitochondria play a crucial role in regulating cell fate decisions by producing ROS and act as redox sensors (Lennicke and Cochemé, 2021). It seems that ERA treatment reduces cystine uptake, which decreases GSH biosynthesis and impairs peroxide detoxification. Therefore, it triggers mitochondrial ROS accumulation (Zhao et al., 2020). It has been shown that RAPA inhibits mTORC1-dependent signaling that can change mitochondrial metabolism and upregulate superoxide generation, particularly when antioxidant systems are compromised (Tao et al., 2025). The combined consideration of ERA and RAPA probably results in a feed-forward loop. Accordingly, mitochondrial ROS damages mitochondrial proteins and lipids, leading to a loss of membrane potential and increased respiratory inefficiency (Wang et al., 2026, Xu et al., 2024). This situation, in turn, further increases ROS levels. Indeed, mitochondrial damage signals activate mitophagy programs (PINK1/Parkin and BNIP3), and extensive organelle turnover that can shift from being protective to lethal when stress persists (De Gaetano et al., 2021). The TOS and TAC results confirm that the intracellular environment becomes more oxidized, especially under ERA + RAPA treatment. The increase in mitochondrial superoxide and TOS suggests that mitochondrial ROS spreads to create a broader oxidative state. The decrease in TAC indicates that antioxidant reserves are depleted or suppressed. This simultaneous rise in oxidants and decline in antioxidants may trigger stress-responsive pathways like autophagy and mitophagy to counteract ROS-induced damage (Mustafa et al., 2025).

In addition, the ERA reduced both GSH/GSSG and NADPH/$NADP^+$ ratios, in line with the expected outcome of system Xc^- inhibition (Wang et al., 2026). In line, limited cystine availability hampers GSH production, leading to a weakened glutathione-dependent detoxification process (Georgiou-Siafis and Tsiftsoglou, 2023). During peroxide detoxification, GSH is oxidized to GSSG, causing a decrease in the GSH/GSSG ratio under oxidative stress conditions (Vairetti et al., 2021). However, the GSH replenishment relies on GR and NADPH (Chandel, 2021). Therefore, a reduction in the NADPH/$NADP^+$ ratio after ERA and RAPA treatment exacerbates the issue by slowing down the regeneration of reduced glutathione. RAPA also reduced these ratios, indicating that inhibiting mTORC1 disrupts the metabolic pathways responsible for maintaining cellular reducing equivalents (Szwed et al., 2021). NADPH production is typically supported by pathways such as the pentose phosphate pathway and $NADP^+$-dependent dehydrogenases (Szwed et al., 2021). mTORC1 inhibition can alter carbon flow and decrease anabolic/antioxidant resources based on nutrient availability and cellular conditions (Fuentes-Lemus et al., 2023).

Furthermore, ERA decreased the activities of GPx, GR, SOD, and CAT, with the most significant suppression observed under co-treatment. This aligns with the observed redox depletion, as SOD and CAT work together to limit ROS accumulation by converting superoxide to H_2O_2 and breaking down H_2O_2 (Afzal et al., 2023, Khalid et al., 2026, Shareef et al., 2026). The decreased activity of these enzymes could increase the superoxide/H_2O_2 levels, especially in mitochondria (Corbeanu and Găman, 2022). GPx and GR play a crucial role in the glutathione cycle for peroxide detoxification and GSH regeneration (Pei et al., 2023, Darweesh and Alnori, 2025). The decreased activity of these enzymes, along with lower levels of NADPH/$NADP^+$ and GSH/GSSG after ERA and RAPA treatment (mainly in combined form),

indicates that the glutathione axis is compromised at various levels, including substrate availability, recycling capacity, and enzymatic activity. A crucial concept to understand is that the decrease in antioxidant enzyme levels can be both a cause and a result of oxidative stress. Oxidative stress can directly deactivate enzymes by oxidizing key residues in their active sites (Chaudhary et al., 2023). In line with this issue, prolonged stress can also hinder protein production and lead to protein breakdown. Furthermore, increased autophagy can break down proteins and organelles, potentially decreasing overall antioxidant defenses (Yun et al., 2020).

The increased levels of PINK1 and Parkin suggest that ubiquitin-dependent mitophagy is activated, which typically occurs when mitochondria lose their membrane potential, and PINK1 accumulates on the outer membrane to recruit Parkin (Barazzuol et al., 2020). The rise in BNIP3 expression also indicates the involvement of receptor-mediated mitophagy, which can be triggered by stress signals such as hypoxia and oxidative damage (Abdrakhmanov et al., 2021). The simultaneous activation of both pathways in this experimental condition suggests a comprehensive response to mitochondrial damage rather than a specific pathway malfunction. The results suggest a sequence of events starting with oxidative stress (increased mitochondrial superoxide, elevated TOS, decreased GSH/NADPH levels), leading to mitochondrial dysfunction and subsequent activation of PINK1/Parkin and BNIP3-mediated recruitment of autophagic machinery. It should be noted that early mitophagy is usually protective, aiming to eliminate ROS-producing mitochondria (Schofield and Schafer, 2021). However, in cases of prolonged redox imbalance (evidenced by reduced TAC, GSH/GSSG levels, and suppressed antioxidant enzymes), excessive mitophagy can lead to excessive removal of mitochondrial mass, resulting in ATP depletion, bioenergetic crisis, and cell death (Zhu et al., 2020). Thus, we can hypothesize that ERA and RAPA in sole and combination shift mitophagy from a compensatory quality-control mechanism toward a maladaptive, death-promoting process when oxidative stress remains unresolved. In line with this hypothesis, LC3-II/LC3-I ratios increased with ERA and RAPA and were highest with the combination. RAPA is expected to enhance autophagy by inhibiting mTORC1 and activating autophagy initiation complexes. ERA-induced oxidative stress can also trigger autophagy as a stress response, including selective organelle turnover (mitophagy).

5. Conclusion

The study showed that ERA and rapamycin (RAPA), either alone or in combination, cause significant redox imbalance and mitochondrial dysfunction in MCF-7 breast cancer cells, leading to a notable decrease in cell viability. ERA disrupted the balance of intracellular thiols, resulting in lower GSH/GSSG and NADPH/$NADP^+$ ratios, reduced activity of GPx, GR, SOD, and CAT, and increased production of mitochondrial superoxide. RAPA also contributed to oxidative stress and increased autophagy. The combined treatment had the most significant impact on oxidative stress, with higher TOS, lower TAC, and impaired antioxidant defense systems. Furthermore, mitochondrial oxidative stress led to the activation of both ubiquitin-dependent (PINK1/Parkin) and receptor-mediated (BNIP3) mitophagy pathways, indicating recognition of mitochondrial damage. The increased LC3-II/LC3-I ratios supported enhanced autophagic activity. Although mitophagy and autophagy are usually protective under mild

stress, the sustained redox collapse in the combined treatment group likely shifted these processes towards excessive mitochondrial clearance, resulting in bioenergetic insufficiency and autophagy-related cell death.

Declarations

Ethical approval

Our research does not involve any human or animal subjects.

Informed consent

Not Applicable, because we worked on cell line

Availability of supporting data

All the data used and analyzed during the current study are available from the corresponding author on reasonable request.

Competing interests

The authors have no conflict of interest to declare.

Funding

The authors declare that no funds, grants, or other support were received during the preparation of this manuscript.

Author contributions

Suhayla Hamad Shareef and Shang Ziyad Abdulqadir performed experiments and revised the manuscript. Lina Abdulfatah Abdulrazaq, Kamal A. Khidir and Adam M. Faraj contributed to the analysis of data, interpretation of data, scientifically to ideas and problem-solving. Ramyar Hassan Mahmud and Hawro Taha Hamza wrote the manuscript and generate ideas. Harem Khdir Awla, Peshraw Salih Hamadamin and Khder H. Rasul provided supervision throughout and wrote the manuscript. All authors have critically reviewed and approved the final draft and are responsible for the content and similarity index of the manuscript.

Acknowledgments

The authors would like to express their sincere gratitude to Department of Biology, College of Science, Salahaddin University-Erbil, Kurdistan Region, Iraq, for their continuous scientific support throughout the course of this study.

References

1. ABDRAKHMANOV, A., YAPRYNTSEVA, M. A., KAMINSKYY, V. O., ZHIVOTOVSKY, B. & GOGVADZE, V. 2021. Receptor-Mediated Mitophagy Rescues Cancer Cells under Hypoxic Conditions. *Cancers (Basel)*, 13.
2. AFZAL, S., ABDUL MANAP, A. S., ATTIQ, A., ALBOKHADAIM, I., KANDEEL, M. & ALHOJAILY, S. M. 2023. From imbalance to impairment: the central role of reactive oxygen species in oxidative stress-induced disorders and therapeutic exploration. *Front Pharmacol*, 14, 1269581.
3. ALHARBI, Y. M., BIMA, A. I. & ELSAMANOUDY, A. Z. 2021. An Overview of the Perspective of Cellular Autophagy: Mechanism, Regulation, and the Role of Autophagy Dysregulation in the Pathogenesis of Diseases. *J Microsc Ultrastruct*, 9, 47–54.
4. BARAZZUOL, L., GIAMOGANTE, F., BRINI, M. & CALÌ, T. 2020. PINK1/Parkin Mediated Mitophagy, Ca(2+) Signalling, and ER-Mitochondria Contacts in Parkinson's Disease. *Int J Mol Sci*, 21.
5. CHANDEL, N. S. 2021. NADPH-The Forgotten Reducing Equivalent. *Cold Spring Harb Perspect Biol*, 13.
6. CHAUDHARY, M. R., CHAUDHARY, S., SHARMA, Y., SINGH, T. A., MISHRA, A. K., SHARMA, S. & MEHDI, M. M. 2023. Aging, oxidative stress and degenerative diseases: mechanisms, complications and emerging therapeutic strategies. *Biogerontology*, 24, 609–662.
7. CHAVEZ-DOMINGUEZ, R., PEREZ-MEDINA, M., LOPEZ-GONZALEZ, J. S., GALICIA-VELASCO, M. & AGUILAR-CAZARES, D. 2020. The Double-Edge Sword of Autophagy in Cancer: From Tumor Suppression to Pro-tumor Activity. *Front Oncol*, 10, 578418.
8. CHEN, X., LI, S., LONG, D., SHAN, J. & LI, Y. 2021. Rapamycin facilitates differentiation of regulatory T cells via enhancement of oxidative phosphorylation. *Cell Immunol*, 365, 104378.
9. CORBEANU, R. I. & GĂMAN, A. M. 2022. The involvement of oxidative stress in non-Hodgkin's lymphomas; a review of the literature. *Journal of Mind and Medical Sciences*, 9, 1.
10. DARWEESH, O. & ALNORI, M. K. 2025. Assessment of Cancer biomarkers and biochemical parameters across breast Cancer stages: Correlation with age and comorbidities. *Cytokine*, 194, 156997.
11. DE GAETANO, A., GIBELLINI, L., ZANINI, G., NASI, M., COSSARIZZA, A. & PINTI, M. 2021. Mitophagy and Oxidative Stress: The Role of Aging. *Antioxidants (Basel)*, 10.
12. FUENTES-LEMUS, E., REYES, J. S., FIGUEROA, J. D., DAVIES, M. J. & LÓPEZ-ALARCÓN, C. 2023. The enzymes of the oxidative phase of the pentose phosphate pathway as targets of reactive species: consequences for NADPH production. *Biochem Soc Trans*, 51, 2173–2187.
13. GEORGIOU-SIAFIS, S. K. & TSIFTSOGLOU, A. S. 2023. The Key Role of GSH in Keeping the Redox Balance in Mammalian Cells: Mechanisms and Significance of GSH in Detoxification via Formation of Conjugates. *Antioxidants (Basel)*, 12.
14. GUO, X., GUO, Y., LI, J., LIU, Q. & WU, H. 2023. Arginine Expedites Erastin-Induced Ferroptosis through Fumarate. *Int J Mol Sci*, 24.

15. JAROCKI, M., TUREK, K., SACZKO, J., TAREK, M. & KULBACKA, J. 2024. Lipids associated with autophagy: mechanisms and therapeutic targets. *Cell Death Discov*, 10, 460.
16. JEE, S. C. & CHEONG, H. 2023. Autophagy/Mitophagy Regulated by Ubiquitination: A Promising Pathway in Cancer Therapeutics. *Cancers (Basel)*, 15.
17. KHALID, Z. S., SULAIMAN, S. R. & RASUL, K. H. 2026. Molecular analysis of FSHR rs6166 polymorphism and oxidative stress parameters in women with polycystic ovary syndrome. *Molecular Biology Reports*, 53, 1055.
18. KOJU, N., QIN, Z. H. & SHENG, R. 2022. Reduced nicotinamide adenine dinucleotide phosphate in redox balance and diseases: a friend or foe? *Acta Pharmacol Sin*, 43, 1889–1904.
19. LENNICKE, C. & COCHEMÉ, H. M. 2021. Redox metabolism: ROS as specific molecular regulators of cell signaling and function. *Mol Cell*, 81, 3691–3707.
20. LI, J., LIU, H., SHAN, Z., ZHONG, K. & LIANG, Q. 2025. Molecular mechanisms and potential implications of ferroptosis, cuproptosis, and disulfidptosis in septic lung injury. *Front Med (Lausanne)*, 12, 1615264.
21. LIU, Y., HU, J., DUAN, X., DING, W., XU, M. & XIONG, Y. 2025. Target of Rapamycin (TOR): A Master Regulator in Plant Growth, Development, and Stress Responses. *Annu Rev Plant Biol*, 76, 341–371.
22. LIU, Y., LU, S., WU, L. L., YANG, L., YANG, L. & WANG, J. 2023. The diversified role of mitochondria in ferroptosis in cancer. *Cell Death Dis*, 14, 519.
23. MA, K., CHEN, G., LI, W., KEPP, O., ZHU, Y. & CHEN, Q. 2020. Mitophagy, Mitochondrial Homeostasis, and Cell Fate. *Front Cell Dev Biol*, 8, 467.
24. MAHEMUTI, D., MA, L., SIDDIQE, W., TANG, Z., KONG, Y., LI, W., ZHANG, Z., SU, Z. & MAIMAITIJIANG, A. 2026. Ferroptosis as a Novel Therapeutic Strategy to Overcome Multidrug Resistance in Colorectal Cancer. *Pharmaceuticals (Basel)*, 19.
25. MOHAMMED, D. S. & SHAREEF, S. H. 2026. Unveiling the novel phytotherapeutic potential of Saussurea costus: Synergistic antiproliferative, antioxidant, and anti-inflammatory pathways against colon cancer in a rat model. *Journal of King Saud University–Science*, 38.
26. MUSTAFA, H. K., RASUL, K. H., ABDULRAHMAN, A. S., AWLA, H. K., MOSHARI, S. & KHIDIR, K. A. 2025. L-Carnitine Attenuates Testicular Dysfunction in Type 1 Diabetes Mellitus Via Modulation of Oxidative Stress, Inflammation, and miRNA Expression. *Inflammation*, 49, 8.
27. PEI, J., PAN, X., WEI, G. & HUA, Y. 2023. Research progress of glutathione peroxidase family (GPX) in redoxidation. *Frontiers in pharmacology*, 14, 1147414.
28. SARıKAYA, E. & DOĞAN, S. 2020. Glutathione Peroxidase in Health. *Glutathione system and oxidative stress in health and disease*, 49.
29. SCHOFIELD, J. H. & SCHAFER, Z. T. 2021. Mitochondrial Reactive Oxygen Species and Mitophagy: A Complex and Nuanced Relationship. *Antioxid Redox Signal*, 34, 517–530.
30. SEMLALI, A., PAPADAKOS, S., CONTANT, C., ZOUAOUI, I. & ROUABHIA, M. 2022. Rapamycin inhibits oral cancer cell growth by promoting oxidative stress and suppressing ERK1/2, NF-κB and beta-

catenin pathways. *Front Oncol*, 12, 873447.

31. SHAREEF, S. H., NANAKALY, H. T., AHMED, S. A., GHENI, N. A., FISAL, D. N., SHAKIR AGHA, N. F. & ABDULLA, M. A. 2026. Astragalin Suppresses Colorectal Carcinogenesis by Targeting Proliferation, Oxidative Stress, and Inflammation. *Cancer Management and Research*, 578138.
32. SREEKUMAR, P. G., FERRINGTON, D. A. & KANNAN, R. 2021. Glutathione Metabolism and the Novel Role of Mitochondrial GSH in Retinal Degeneration. *Antioxidants (Basel)*, 10.
33. SUN, Y., DENG, R. & ZHANG, C. 2020. Erastin induces apoptotic and ferroptotic cell death by inducing ROS accumulation by causing mitochondrial dysfunction in gastric cancer cell HGC–27. *Mol Med Rep*, 22, 2826–2832.
34. SWANDA, R. V., JI, Q., WU, X., YAN, J., DONG, L., MAO, Y., UEMATSU, S., DONG, Y. & QIAN, S. B. 2023. Lysosomal cystine governs ferroptosis sensitivity in cancer via cysteine stress response. *Mol Cell*, 83, 3347–3359.e9.
35. SZWED, A., KIM, E. & JACINTO, E. 2021. Regulation and metabolic functions of mTORC1 and mTORC2. *Physiol Rev*, 101, 1371–1426.
36. TAO, D., XIA, Y., LIAO, Q., YANG, X., ZHANG, L. & XIE, C. 2025. Rapamycin mitigates neurotoxicity of fluoride and aluminum by activating autophagy through the AMPK/mTOR/ULK1 pathway in hippocampal neurons and NG108-15 cells. *Sci Rep*, 15, 9801.
37. VAIRETTI, M., DI PASQUA, L. G., CAGNA, M., RICHELMI, P., FERRIGNO, A. & BERARDO, C. 2021. Changes in Glutathione Content in Liver Diseases: An Update. *Antioxidants (Basel)*, 10.
38. VARGAS, J. N. S., HAMASAKI, M., KAWABATA, T., YOULE, R. J. & YOSHIMORI, T. 2023. The mechanisms and roles of selective autophagy in mammals. *Nat Rev Mol Cell Biol*, 24, 167–185.
39. WANG, B., WANG, Y., ZHANG, J., HU, C., JIANG, J., LI, Y. & PENG, Z. 2023. ROS-induced lipid peroxidation modulates cell death outcome: mechanisms behind apoptosis, autophagy, and ferroptosis. *Arch Toxicol*, 97, 1439–1451.
40. WANG, H., CHENG, Y., MAO, C., LIU, S., XIAO, D., HUANG, J. & TAO, Y. 2021. Emerging mechanisms and targeted therapy of ferroptosis in cancer. *Mol Ther*, 29, 2185–2208.
41. WANG, K., WANG, H., ZHANG, Y., ZHANG, Z., WANG, L., YANG, J., MAN, J. & YANG, L. 2026. Reprogramming mitochondrial homeostasis in renal ischemia-reperfusion injury. *Cell Signal*, 139, 112294.
42. WANG, L., LIU, Y., DU, T., YANG, H., LEI, L., GUO, M., DING, H. F., ZHANG, J., WANG, H., CHEN, X. & YAN, C. 2020. ATF3 promotes erastin-induced ferroptosis by suppressing system Xc(). *Cell Death Differ*, 27, 662–675.
43. WU, P., WANG, A., CHENG, J., CHEN, L., PAN, Y., LI, H., ZHANG, Q., ZHANG, J., CHU, W. & ZHANG, J. 2020. Effects of Starvation on Antioxidant-Related Signaling Molecules, Oxidative Stress, and Autophagy in Juvenile Chinese Perch Skeletal Muscle. *Mar Biotechnol (NY)*, 22, 81–93.
44. XIAO, W. & LOSCALZO, J. 2020. Metabolic Responses to Reductive Stress. *Antioxid Redox Signal*, 32, 1330–1347.

45. XU, M., FENG, P., YAN, J. & LI, L. 2024. Mitochondrial quality control: a pathophysiological mechanism and potential therapeutic target for chronic obstructive pulmonary disease. *Front Pharmacol*, 15, 1474310.
46. YAMASHITA, S. I., SUGIURA, Y., MATSUOKA, Y., MAEDA, R., INOUE, K., FURUKAWA, K., FUKUDA, T., CHAN, D. C. & KANKI, T. 2024. Mitophagy mediated by BNIP3 and NIX protects against ferroptosis by downregulating mitochondrial reactive oxygen species. *Cell Death Differ*, 31, 651–661.
47. YANG, Y., AN, Y., REN, M., WANG, H., BAI, J., DU, W. & KONG, D. 2023. The mechanisms of action of mitochondrial targeting agents in cancer: inhibiting oxidative phosphorylation and inducing apoptosis. *Front Pharmacol*, 14, 1243613.
48. YUN, H. R., JO, Y. H., KIM, J., SHIN, Y., KIM, S. S. & CHOI, T. G. 2020. Roles of autophagy in oxidative stress. *International journal of molecular sciences*, 21, 3289.
49. ZANDI, P. & SCHNUG, E. 2022. Reactive Oxygen Species, Antioxidant Responses and Implications from a Microbial Modulation Perspective. *Biology (Basel)*, 11.
50. ZHAO, Y., LI, Y., ZHANG, R., WANG, F., WANG, T. & JIAO, Y. 2020. The Role of Erastin in Ferroptosis and Its Prospects in Cancer Therapy. *Onco Targets Ther*, 13, 5429–5441.
51. ZHOU, T. Y., MA, R. X., LI, J., ZOU, B., YANG, H., MA, R. Y., WU, Z. Q., LI, J. & YAO, Y. 2023. Review of PINK1-Parkin-mediated mitochondrial autophagy in Alzheimer's disease. *Eur J Pharmacol*, 959, 176057.
52. ZHU, Y. X., JIA, H. R., GAO, G., PAN, G. Y., JIANG, Y. W., LI, P., ZHOU, N., LI, C., SHE, C., ULRICH, N. W., CHEN, Z. & WU, F. G. 2020. Mitochondria-acting nanomicelles for destruction of cancer cells via excessive mitophagy/autophagy-driven lethal energy depletion and phototherapy. *Biomaterials*, 232, 119668.

Figures

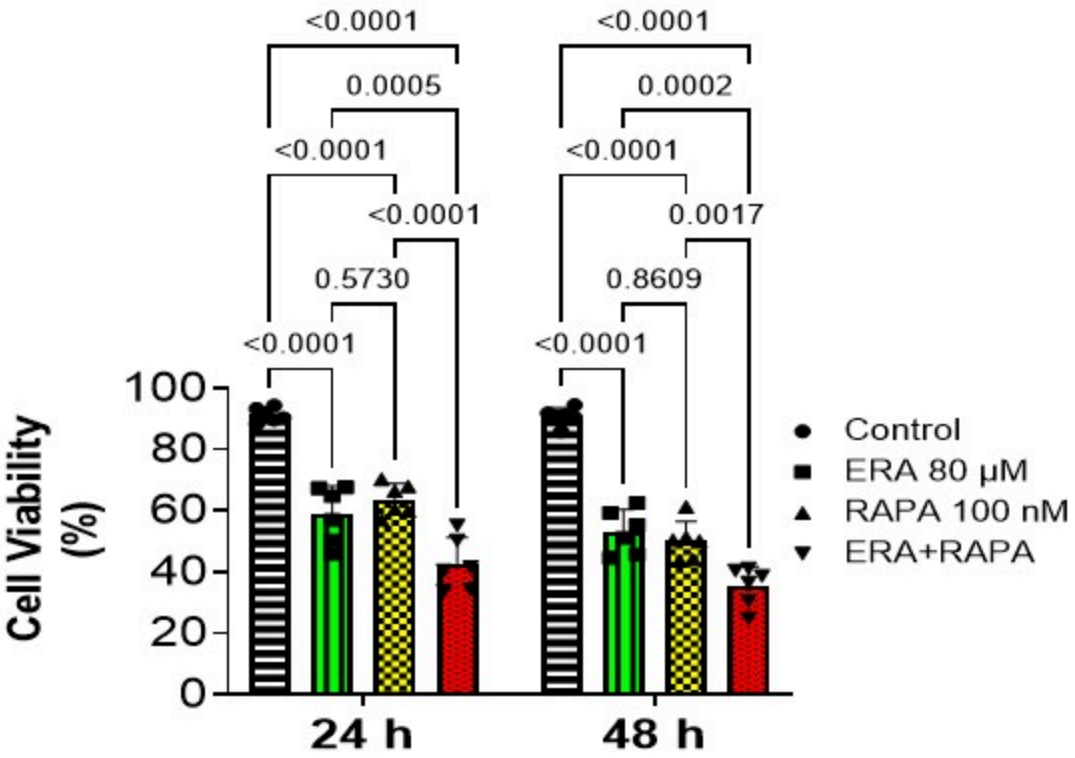

Figure 1

MTT analysis for MCF7 cell viability after ERA and RAPA in sole and co-treatment conditions. All data are presented in Mean ±SD (n=6/group).

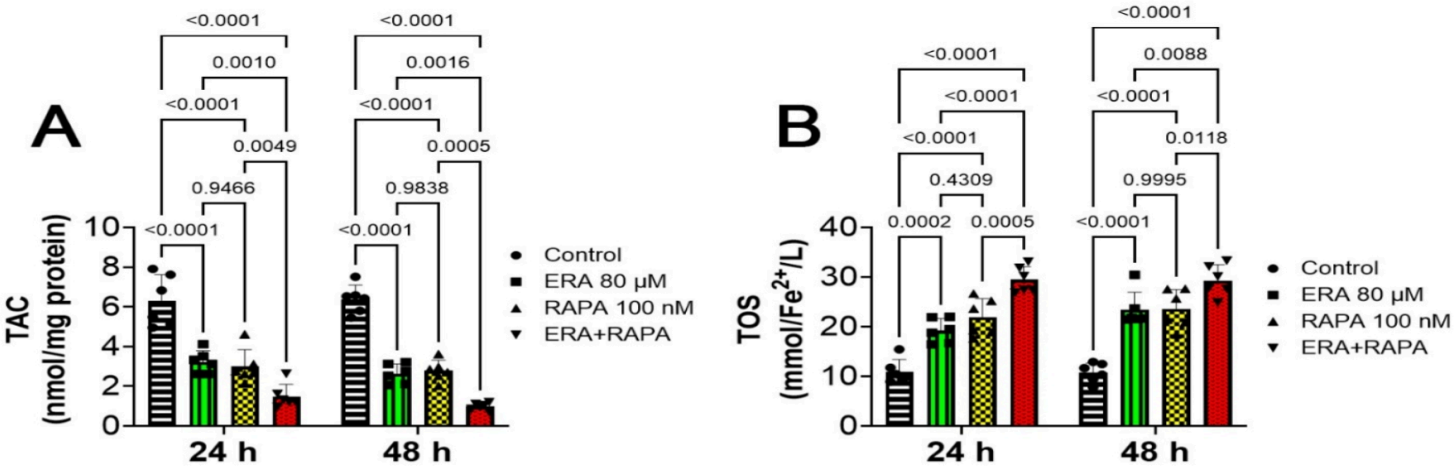

Figure 2

Effects of ERA and RAPA in sole and co-treatment conditions on (A) TAC and (B) TOS in MCF-7 cell line. All data are presented in Mean ±SD (n=6/group).

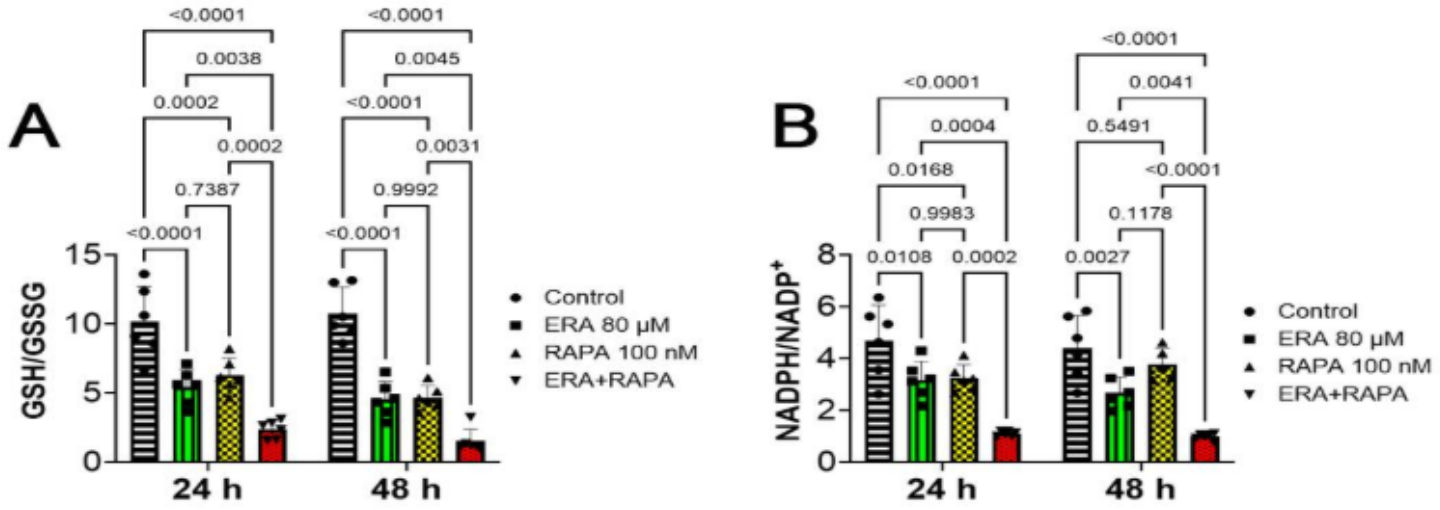

Figure 3

Effects of ERA and RAPA in sole and co-treatment conditions on (A) GSH/GSSG ratio and (B) NADPH/NADP+ ratio in MCF-7 cell line. All data are presented in Mean±SD (n=6/group).

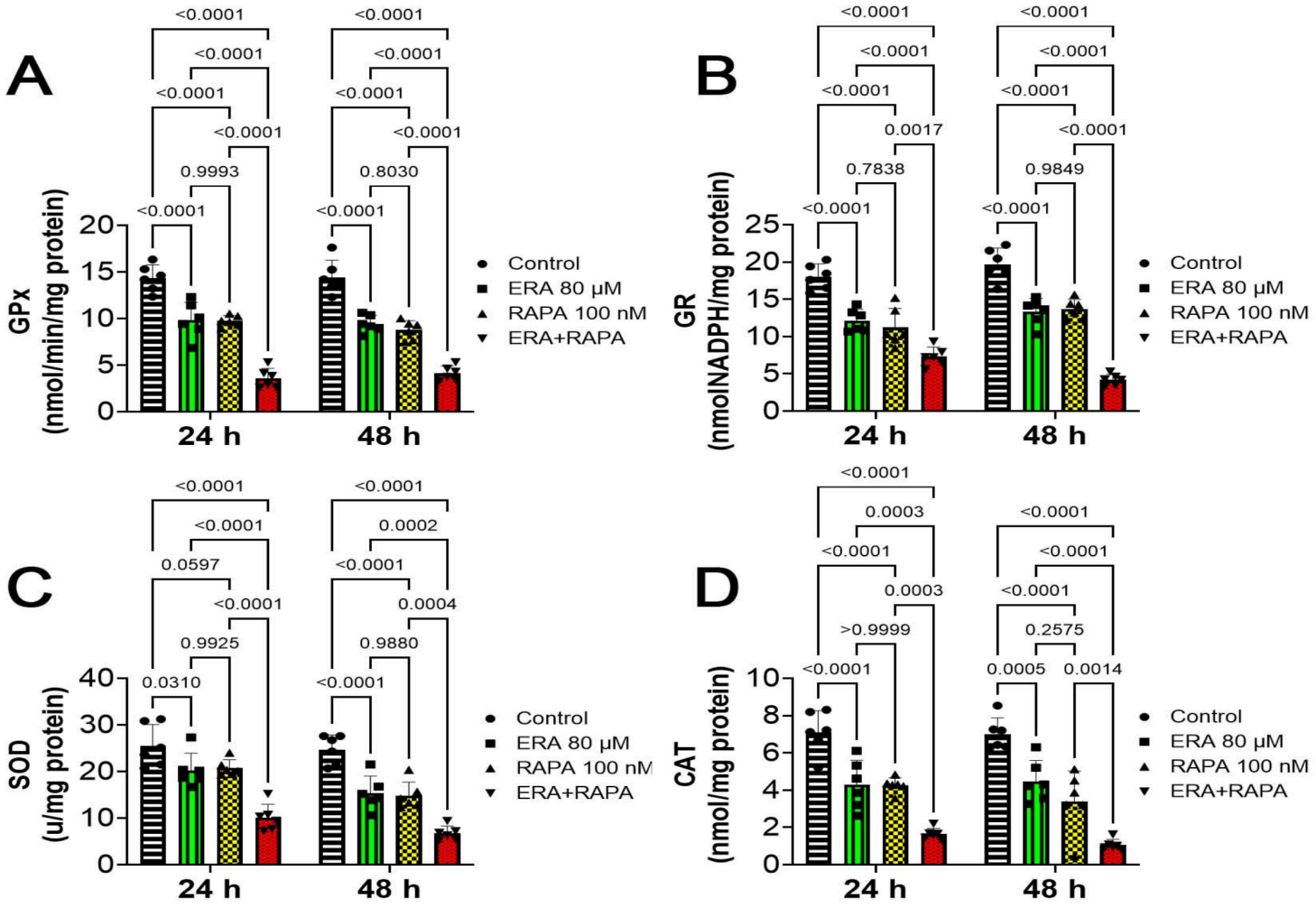

Figure 4

Effects of ERA and RAPA in sole and co-treatment conditions on (A) GPx, (B) GR, (C) SOD, and (D) CAT levels in MCF7 cell line. All data are presented in Mean±SD (n=6/group).

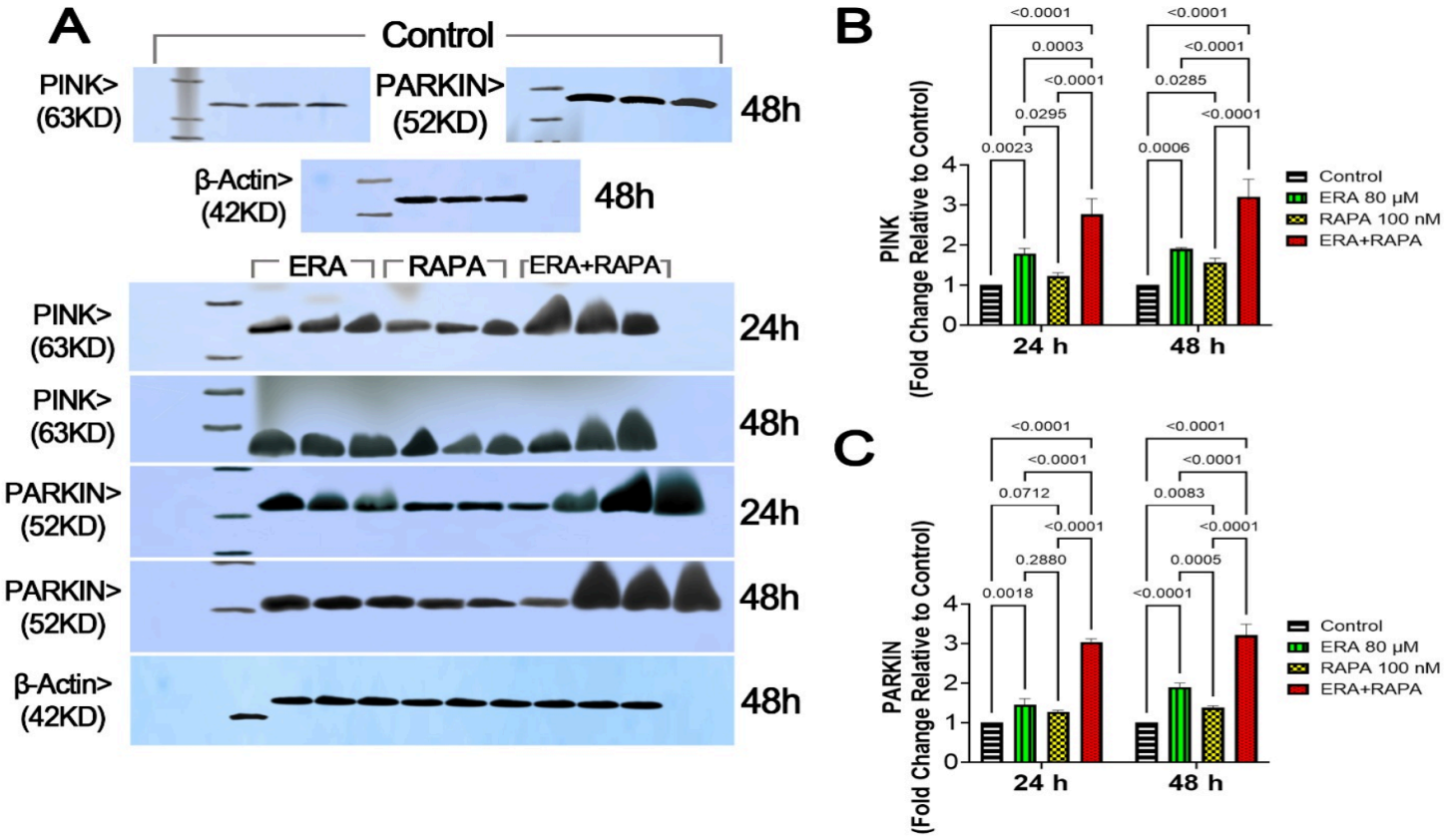

Figure 5

Effects of ERA and RAPA in sole and co-treatment conditions on PINK and PARKIN expression levels in MCF7 cell line. (A) western blot photomicrographs, (B) PINK protein fold change relative to control group, and (C) PARKIN protein fold change relative to control group. All data are presented in Mean±SD (n=6/group).

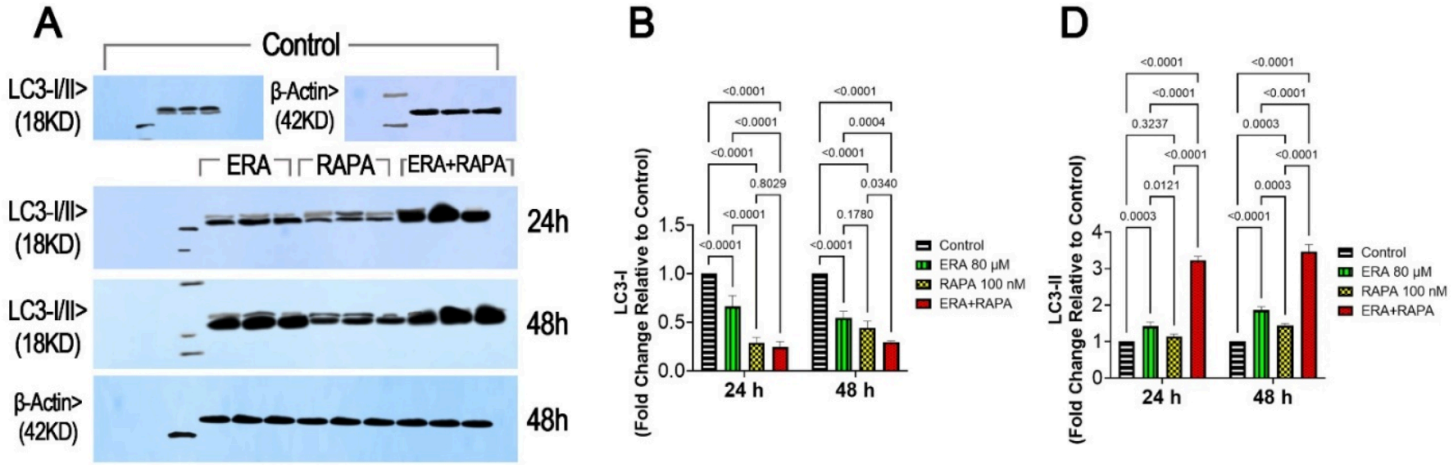

Figure 6

Effects of ERA and RAPA in sole and co-treatment conditions on LC3-I and LC3-II expression levels in MCF7 cell line. (A) western blot photomicrographs, (B) LC3-I protein fold change relative to control group, and (C) LC3-II protein fold change relative to control group. All data are presented in Mean±SD (n=6/group).

Supplementary Files

This is a list of supplementary files associated with this preprint. Click to download.

- Supplementaryfile.pdf